

LOAN DOCUMENT

DTIC ACCESSION NUMBER		PHOTOGRAPH THIS SHEET	INVENTORY												
		LEVEL	(0)												
<p><i>MEMS Actuated Deployable Flow Effectors . . .</i></p> <p>DOCUMENT IDENTIFICATION 2000</p>															
<p>DISTRIBUTION STATEMENT A Approved for Public Release Distribution Unlimited</p>															
<p>ACCESSION FOR</p> <table border="1" style="width: 100%; border-collapse: collapse;"><tr><td style="width: 50%;">NTIS</td><td style="width: 50%;">GRAM</td></tr><tr><td>DTIC</td><td>TRAC</td></tr><tr><td>UNANNOUNCED</td><td></td></tr><tr><td>JUSTIFICATION</td><td></td></tr></table> <p>BY</p> <p>DISTRIBUTION/</p> <p>AVAILABILITY CODES</p> <table border="1" style="width: 100%; border-collapse: collapse;"><tr><td style="width: 50%;">DISTRIBUTION</td><td style="width: 50%;">AVAILABILITY AND/OR SPECIAL</td></tr><tr><td style="height: 50px; vertical-align: middle; font-size: 2em;">A-1</td><td></td></tr></table>		NTIS	GRAM	DTIC	TRAC	UNANNOUNCED		JUSTIFICATION		DISTRIBUTION	AVAILABILITY AND/OR SPECIAL	A-1		<p>DISTRIBUTION STATEMENT</p>	
		NTIS	GRAM												
DTIC	TRAC														
UNANNOUNCED															
JUSTIFICATION															
DISTRIBUTION	AVAILABILITY AND/OR SPECIAL														
A-1															
<p>DISTRIBUTION STAMP</p>		<p>DATE ACCESSIONED</p>													
		<p>DATE RETURNED</p>													
<p style="font-size: 2em;">20010201 063</p>		<p>REGISTERED OR CERTIFIED NUMBER</p>													
<p>DATE RECEIVED IN DTIC</p>															
<p>PHOTOGRAPH THIS SHEET AND RETURN TO DTIC-FDAC</p>															

H
A
N
D
L
E

W
I
T
H

C
A
R
E

MEMS ACTUATED DEPLOYABLE FLOW EFFECTORS SYSTEM FOR MISSILE CONTROL

Mehul P. Patel

*Aerodynamics Engineer
Orbital Research Inc., Cleveland, OH 44143*

T. Terry Ng

*Professor of Mechanical Engineering
University of Toledo, Toledo, OH 43606*

Frederick J. Lisy

*Vice President
Orbital Research Inc., Cleveland, OH 44143*

Troy S. Prince

*Systems and Controls Engineer
Orbital Research Inc., Cleveland, OH 44143*

Jack M. DiCocco

*Aerospace Engineer
Orbital Research Inc., Cleveland, OH 44143*

ABSTRACT

This paper presents an innovative active flow control strategy to enhance missile launch capability and increase maneuverability of missiles at high Angle of Attack [α] thereby allowing rear hemisphere engagement maneuvers. This flow control technique utilizes Deployable Flow Effectors [DFE's], which can be actuated using miniature pneumatic valves or micropumps that are fabricated using MicroElectroMechanical Systems [MEMS] technology. Low power pressure sensors are integrated with the DFE's in a common fixture called a Co-Located Actuator and Sensor [CLAS] unit. Additionally, the CLAS unit is integrated into a 3:1 tangent ogive nosecone of a 57% scale model of a typical Air-to-Air Missile. This CLAS configuration enables high sensor spatial resolution and optimal placement of flow effectors and sensors on the missile forebody.

DFE effectiveness is measured and quantified by pressure, force balance, and flow visualization. By controlling vortex shedding from the slender body at high α , effective control of induced yawing moments can be achieved using the DFE's. Further, time-frequency analysis of dynamic pressure data demonstrated the ability to determine 'optimal' DFE configuration.

Introduction

Both slender bodies and aircraft oriented at high α are subject to large side forces (or yawing tendencies) caused by asymmetric flow separation and vortex shedding. Significant decrease in control, maneuverability, and intense vibrations are often the result of such flow conditions¹. However, recent aerodynamic studies and simulations have shown that superior aerial combat advantage can be obtained through competitive maneuvering at high α ¹.

Angle of attacks ranging from 0° to 90° for a slender body can be broken into three conditions: low ($0 \leq \alpha < \alpha_{\text{Symmetric Vortices}}$), intermediate ($\alpha_{\text{Symmetric Vortices}} \leq \alpha \leq \alpha_{\text{Asymmetric Vortices}}$), and high ($\alpha_{\text{Asymmetric Vortices}} \leq \alpha \leq \alpha_{\text{Unsteady Vortices}}$)². Significant asymmetric vortices are generated at high angles of attack². Asymmetric vortex shedding on a slender body at high α is caused by uneven flow separation from the nosecone. Many researchers have concluded that this aerodynamic problem results from micro-asymmetries on the surface of the nosecone such as small dents, cracks in the paint, and other microscopic imperfections near the tip of the nosecone³. It has been shown that these asymmetries are affected by the following parameters¹: bluntness of the forebody, Reynolds number, roll angle, and, the angle of attack. Thus, it is possible to alter effective yawing moments on a slender body at high α by controlling forebody flow

Unclassified

separation. The asymmetric vortex shedding from slender bodies and aircraft maneuvering at high α causes significant induced yawing moments due to the pressure differentials across the body, thereby limiting the angle of attack range of the air vehicle. Elimination or reduction of asymmetric vortex shedding will reduce the effective yawing moment on the body. This effective yawing moment caused by asymmetric vortex shedding at high α is often referred to as phantom yaw.

One goal of flow control research on missiles has been to eliminate or reduce the asymmetric separation of flow off the nosecone. Flow control methods that have demonstrated with limited success include; 1) varying the nosecone shape, 2) longitudinal passive strakes near the nosecone tip, 3) spinning the nosecone up to 100 rpm, and 4) passive boundary layer transition strips³.

Recent tests performed under the Enhanced Fighter Maneuverability [EFM] program utilized boundary layer transition strips and strakes placed symmetrically on the fore bodies of both X-31 and F-18³. The purpose of the transition strips and strakes is to ensure that the laminar boundary layer would transition to a turbulent boundary layer at the same locations on both sides of the nosecone. Tests done with the transition strips in place showed an increase in the magnitude of the asymmetry and an occurrence over a wider range of α ³. During the F-18 HARV [High Alpha Research Vehicle] tests, it is found that despite the transition strips, the F-18 HARV experienced intense wing rock at $\alpha=45^\circ$. Tests are performed on a standard F-18 that is known to have nose yawing tendencies at $\alpha=50^\circ$. Transition strips are found to be ineffective in correcting flow asymmetries at $\alpha=50^\circ$, yet effective at $\alpha=60^\circ$. After the F-18 flight tests, both test pilots commented that "the boundary transition strips did not improve the high α qualities of the aircraft"³. This demonstrates the limitations of passive flow control techniques on asymmetric vortex shedding at high α .

Ho at UCLA has investigated the use of silicon based cantilever tabs on the surface of airfoils as means of controlling airflow

over aerodynamic surfaces⁴. Carman⁵ at UCLA has been developing SMA based micro-bubble actuators for flow control. Other types of MEMS actuators include piezo electric devices that are limited by extremely small throws, and magnetostrictive materials that are also limited by need for large external magnetic fields. The heat generated by SMA alloy devices or the magnetic fields needed for magnetostrictive devices may reduce vehicle stealthiness and in the case of missile interfere with radar and infrared seekers.

Despite the promise of MEMS based actuators and sensors, there remain numerous limitations on their use. The challenges facing MEMS devices on aerodynamic surfaces are:

1. A need to protect devices from the environment (temperature, rain, snow, ice)
2. The inherent fragility of the MEMS devices.
3. Insufficient throws and
4. Interfacing constraints such as power and size.
5. The temperature change (above 200°C) while accelerating into the transonic environment will be hard to withstand for most silicon devices and commercially available SMAs.

To address many of these problems, ORI has developed a technique to imbed the MEMS device beneath the surface of the aerodynamic surface. Embedding the MEMS actuators beneath the surface protects the device from the environment, while only marginally increasing system volume requirements, and retaining the advantages of MEMS devices.

This paper presents a novel approach to manipulate and control the asymmetric vortices off the forebody of a missile based on MEMS actuated DFE's system tested on a 57% scale model of a typical Air-to-Air Missile with a 3:1 tangent ogive nose cone. The CLAS module integrated into the missile forebody successfully demonstrated effectiveness in controlling vortex shedding and reducing the phantom yaw on the missile body. Control through vortex stabilization and manipulation at high α will increase launch capabilities and the maneuverability of missiles.

Deployable Flow Effectors [DFE's] Actuator System

The proposed Deployable Flow Effector (DFE) system is based around a circular ring with integrated Co-Located Actuators and Sensors (CLAS). The CLAS ring has low power pressure sensors co-located with pneumatically deployed flow effectors. A circular ring is necessary due to the rolling of the missile in flight which prevents choosing a single set of locations for the sensors and actuators. The ring is designed to be located near the nose of the missile to improve performance and reduce the impact of the actuators on a missile sensor suite. A picture of the 57% scale model of a typical Air-to-Air Missile is shown in **Figure 1**.

There are eight individual actuators arrayed around the surface of the CLAS ring. Each of the DFE's in the test system are pneumatically actuated (10 psi required for full actuation) with conventional micro-valves. The system is designed to allow the integration of Orbital Research Inc. MEMS fabricated microvalves to further reduce the volume required for the DFE structure. When retracted each DFE is flush against the surface to reduce drag and flow effects when not in use.

Co-Located with each actuator is a small dynamic pressure sensor. An inexpensive and sensitive miniature pressure sensor, the Omega PX70 series differential pressure sensor with an operating range of 0-0.3 psi is integrated with the actuator inside each CLAS ring. Measurements from each pressure sensor is filtered and amplified within the wind tunnel model with frequency tunable low-pass filter-amplifiers integrated onto a single printed circuit board with drive electronics for the micro-valves. These pressure sensors are used for two purposes. The first purpose is to determine where the flow is separating from the surface. This information can be



Figure 1(a). A photograph of the 3:1 tangent ogive nose cone.

used to determine which orientation the missile is in while flying without any external information, thereby determining which flow effectors to use at any given time. The second purpose of the pressure sensors is to determine the pressure distribution over the surface of the missile, which may be used as a feedback signal for a yawing moment feedback controller.

Wind Tunnel Test Model

The CLAS ring is tested in a 57% scale model of a typical Air-to-Air Missile with a 3:1 tangent ogive nosecone; see **Figure 2**. In addition to the dynamic pressure sensors, the model is outfitted with four rings of 32 each, PSI™ scanned pressure taps to take body pressure measurements. Surface pressure distributions on aerodynamic models are measured using PSI 32-port electronic pressure scanners. The fast response-rate and rapid scanning capability of the scanner allow time-resolved measurements of unsteady flows. The model is mounted to the wind tunnel with a stinger equipped with four strain gages to form a pitch and yaw moment measurement system. All data is collected on a pair of personal computer (PC) based data acquisition systems running LabView. Additional flow information is gathered using smoke and laser sheet flow visualization techniques.

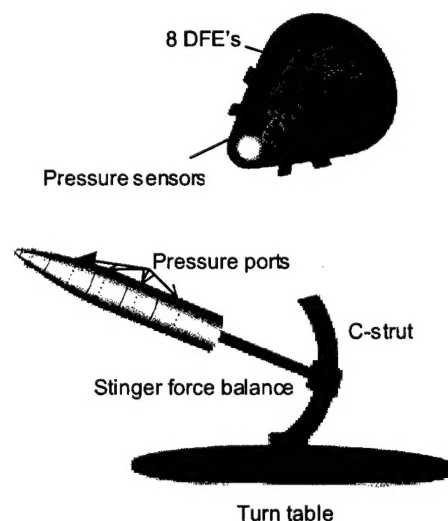


Figure 2. Schematic of Missile nose cone setup

Test Facility

The missile is a 57% scale model of an a typical Air-to-Air Missile with a 3:1 tangent ogive nose cone (see Figure 1). The length of the nose cone is 11.45". The wind tunnel tests are performed at The University of Toledo, Fluid Dynamics Laboratory in the 3' x 3' closed-loop low-speed wind tunnel. The model support incorporates a turntable, a C-strut, and a round-sting mount to allow independent variations of pitch, yaw, and roll angles (see Figure 2). A motor is incorporated into the turntable drive to facilitate remote model positioning. The flow in the test-section is uniform, with a turbulence level of about 0.2% outside of the wall boundary layers. Two pc's and electronic instrumentation are utilized for pressure measurements and data acquisition and calculations.

Data Acquisition

The data acquisition system consists of a computer equipped with a National Instruments data acquisition board and a multiplexer board. The system provides up to 64 single-ended analog-to-digital channels, 8 digital I/O lines, 2 digital-to-analog outputs, signal conditioning, and a host of triggers and clocks. A LabVIEW software package from National Instruments allows rapid code development. Data can be reduced on-line, or stored on removable hard disks for later processing. Data can be processed with the computers in the laboratory or transferred electronically to the other university computing facilities.

Wind Tunnel Experiments

The missile model is tested with dynamic pressures of 5Q, approximately 190 ft/s (130 mph). The model is tested from 20° to 65° α in increments of 5°. Two sets of wind tunnel experiments are conducted on the 57% scaled Air-to-Air Missile model. The first set of experiment is used to empirically optimize the best flow effector configuration while the second set is used to quantify the overall effectiveness of the CLAS ring of flow effectors.

The first set of experiments, conducted prior to the design of the CLAS ring for the DFE's, is used to experimentally optimize the design and configuration of the DFE's for use in the CLAS ring. Four

different configurations of active flow control devices are tested at various deployment heights. Each flow control device is able to be rotated the entire circumference of the missile to allow the orientation of the flow effector to the incident flow to be rapidly changed. The four different active flow control device configurations are: (1) Single square flow effector located 1.3" from the nose; (2) a strake located 2.55" from the nose; (3) a row of four square flow effectors starting 2.55" from the nose (see Figure 3).

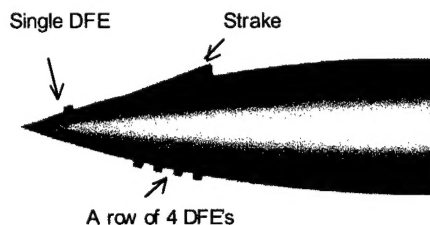


Figure 3. Single FE, a strake and a row of 4 FE on the missile model (not to scale).

The experimental procedure for the first set of tests started with baseline testing of the clean model with no flow control devices. Thereafter, passive flow control devices experiments are performed to evaluate the performance of the DFE's. After determining the most effective passive flow control device to increase missile stability and enhance missile maneuverability, active DFE's are designed from the optimum passive flow control device. With the active DFE's, cycling tests of the flow effectors are done to determine an increase in its effectiveness. The objective of the first set of experiments is to determine and characterize the best flow effector configuration. Effects of different sizes, shapes and location of the flow effector on the nose cone are studied to determine the optimal design of the CLAS units. The effect of deploying the flow effector statically and also at varying frequencies is studied to identify the most favorable flow effector. Again, the most favorable flow effector is determined from the force balance data. The largest moment produced in the desired location by the DFE configuration is then scrutinized for optimal configuration at the given flow conditions.

The second set of experiments utilized the CLAS ring described above using the empirically optimized flow effector design from the first set of testing (see figure 2). The tests ranged from $\alpha = 25^\circ$ to 65° with increments of 5° . In the second set of experiments, 8 DFE's are integrated with 8 Omega PX70 series differential pressure sensors in a CLAS unit and is placed in the nose cone based on the optimal CLAS unit location and configuration from the first set of experiments (see figure 5). The tests ranged from statically deploying each of them to dynamic deployment of 8 DFE's at varying frequencies. The most effective DFE's are then deployed statically and also at varying frequencies in a batch to obtain increased effectiveness. This second set of experiments is conducted recently and the effects of the DFE's are currently being quantified and undergoing investigation. Pressures on the model, force balance measurements and flow visualization are observed and recorded to determine the missile's aerodynamic characteristics.

CLAS Module DFE Testing Data – Passive Wind Tunnel Test

The first sets of passive data is generated to optimize the design of the DFE's. From the first sets of experiments, the performance of each flow effector (strakes and vortex generators located on forebody 2 hatches, and single generator located at the forebody 1 hatch at two different heights) compared to the baseline at $50^\circ \alpha$ is shown in **Table 1**.

Table 1 shows that the baseline model has a natural asymmetric bias force in the

negative direction. Deploying any of the flow effectors produces a force in the opposite direction indicating the reversal of the natural asymmetric vortex formed by model irregularities. The flow effectors mounted on the forebody 2 sections are also capable of reversing the effective yawing moment on the missile model, but to a lesser extent than the forebody 1 flow effector. The flow effector mounted on the forebody 1 section is found to produce the maximum force when deployed.

Figure 4 shows the pressure distribution around the circumference of the slender body for the baseline model, and the effect of deploying both the vortex generators and the strakes from the forebody 2 port at 70° CBP. This figure indicates the pressure distribution around the missile nose cone. It shows the attainable forces that can be generated by a ring of actuators.

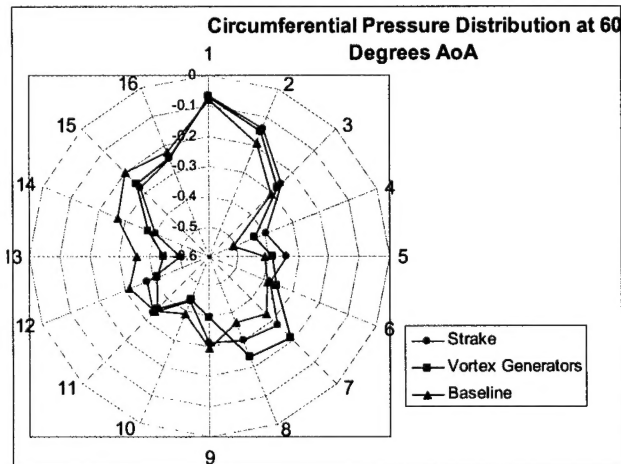


Figure 4. Circumferential Pressure Distribution at $60^\circ \alpha$ for the Model Baseline, with Vortex Generators at 70° CBP, and with Stakes at 70°

Effective Force	Flow Effector Type
1.32 lbs	Strake Forebody 2: 3 mm Deployment @ 70° CBP
1.30 lbs	Vortex Generators Forebody 2: 2-4 mm Deployment @ 70° CBP
0.60 lbs	Strake Forebody 1: 1.5 mm Deployment @ 70° CBP
1.64 lbs	Strake Forebody 1: 3.75 mm Deployment @ 120° CBP
0.72 lbs	Baseline: Natural Model Asymmetry

Table 1 Effective Yawing Force of Deployable Flow Effectors at $50^\circ \alpha$.

Active Wind Tunnel Test

The performance of the DFE's from the second sets of experiments at α ranging from 25° - 60° compared to the baseline configuration with no flow effectors is quantified here forth. Figure 5 show the

effective moment generated by DFE's in Nm. versus α ranging from 25° to 60° . At each α , all the 8 DFE's are actuated discretely and the effect of each is observed. 2 DFE's are then selected at each α that generated the maximum force in the opposite direction as shown in figure 5. Table 2 lists the flow effectors that are deployed at the corresponding angles of attack. As α increases, the overall effectiveness if the DFE's also increases. This is significant for aerodynamic control surfaces for they tend to lose their effectiveness at high α .

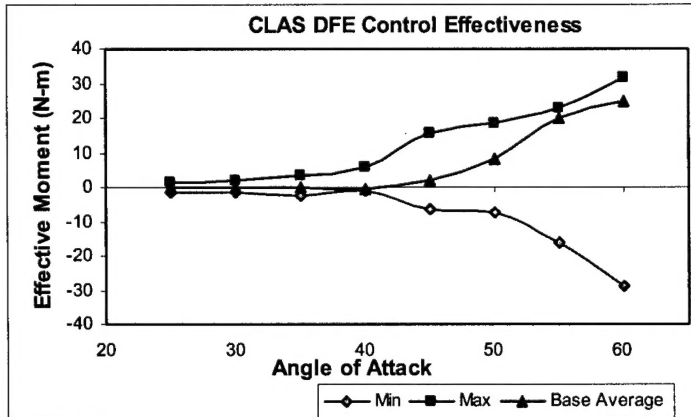


Figure 5. Effective force in N-m vs. Angle of attack [25° - 60°]

AoA	Deployed FE #
	Max(+), Min(-)
25	0, 6
30	0, 6
35	0, 6
40	0, 6
45	1, 6
50	1, 6
55	1, 5
60	1, 5

a

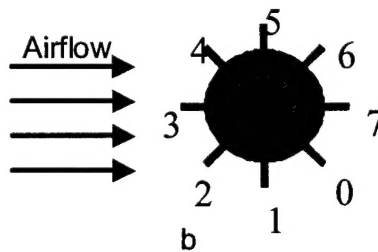


Table 2. (a) Deployed Flow effectors at corresponding Angle of attack (b) DFE# configuration on the missile model (not to scale).

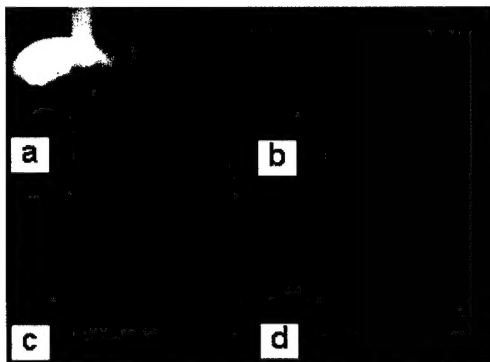


Figure 6. Laser sheet flow visualization at $\alpha = 60^\circ$. (a) Normal view of Missile model (b) Baseline with no DFE (c) DFE #5 actuated (d) DFE #1 actuated.

Static Deployment of the DFE's produces tangible changes in effective moment on the slender body thereby demonstrating that the asymmetric vortices are switched. Laser sheet flow visualization of the flow effectors demonstrated vortex reversal; see Figure 6. Figure 6(a) is shown for a better understanding of the model orientation for flow visualization. Figure 6 (b), (c), and (d) shows the flow visualization with no flow effector deployed, flow effector # 5 deployed and flow effector #1 deployed respectively. Flow effectors 1 and 5 are located diametrically opposite, hence the switching of vortices in the opposite direction compared to the baseline.

It is observed that as α increases, the overall effectiveness of the DFE's also increases. Cycling of the deployable flow control devices can be used to modulate the overall control authority. Figure 7-10 shows a smooth [sic] continuum of effective mean yawing moment applied to the missile model achieved by cycling the flow control devices.

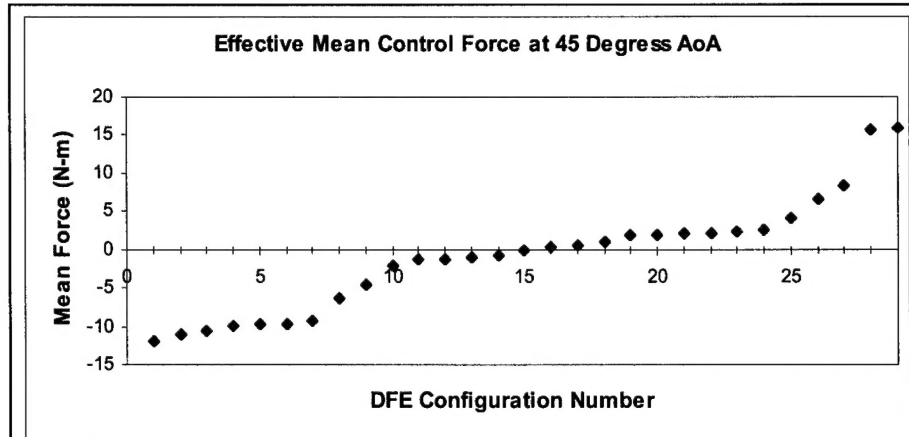


Figure 7. – Effective Mean Force in N-m vs. DFE configuration number for $\alpha = 45^\circ$ as listed in table 3.

DFE Config. Number	Flow Effector 1 Frequency*	Flow Effector 6 Frequency*	Mean Yawing Moment (N-M)
1	x	11	-11.9
2	x	17	-11.0
3	x	20	-10.6
4	x	8	-9.8
5	x	5	-9.8
6	x	14	-9.6
7	x	2	-9.2
8	0	x	-6.4
9	6	1	-4.6
10	3	16	-2.0
11	15	4	-1.3
12	1	5	-1.1
13	12	9	-1.0
14	2	x	-0.8
15	17	12	-0.2
16	17	15	0.4
17	10	16	0.6
18	12	19	1.1
19	19	15	1.9
20	16	15	2.0
21	14	x	2.2
22	17	x	2.2
23	5	x	2.4
24	11	1	2.6
25	20	x	4.3
26	11	x	6.6
27	x	x	8.4
28	x	0	15.7
29	8	x	15.9

*x - indicates that the flow effector is completely retracted

*0 - indicates that the flow effector is statically deployed

*# - indicates that the listed flow effector is deployed at n cycles/sec

Table 3. DFE configuration number key showing deployed flow effectors in position 1 and 6 at varying frequencies and the resultant mean yawing moment generated by that configuration

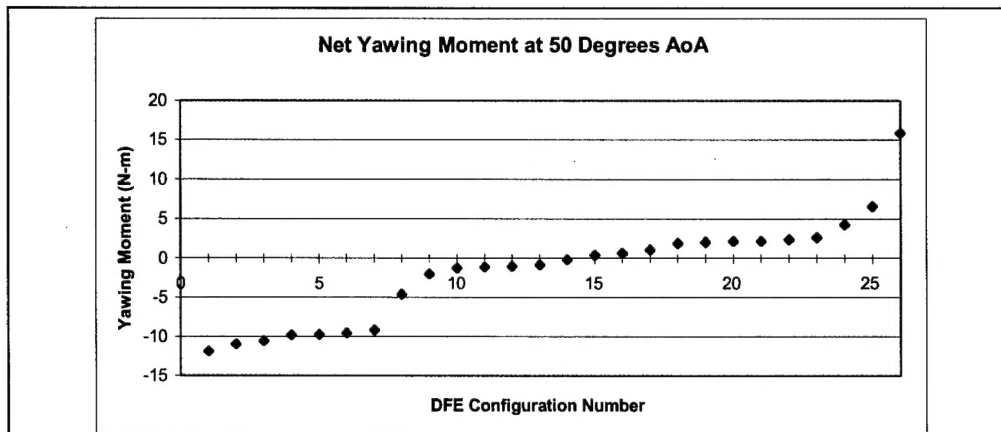


Figure 8. – Effective Mean Force vs. DFE configuration number for $\alpha = 50^\circ$ as listed in table 3.

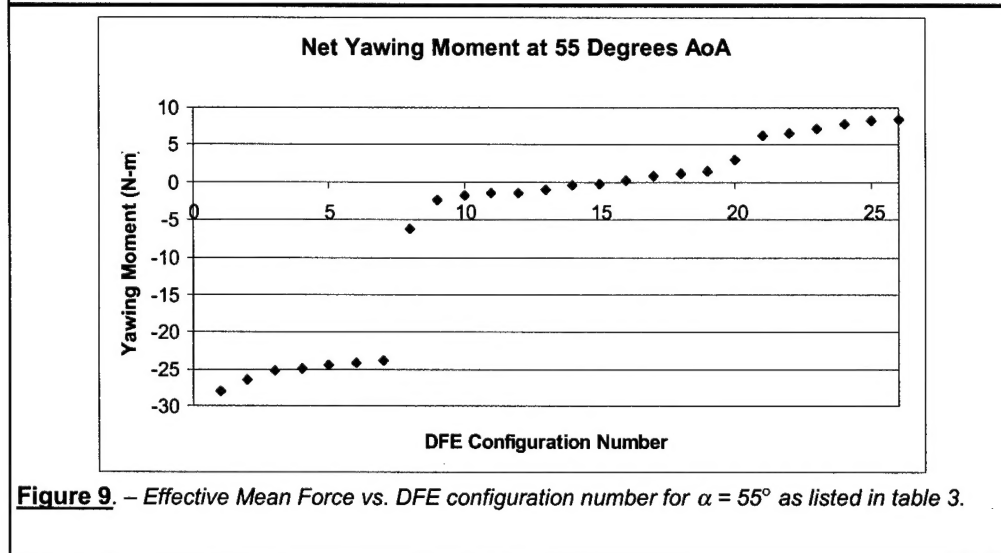


Figure 9. – Effective Mean Force vs. DFE configuration number for $\alpha = 55^\circ$ as listed in table 3.

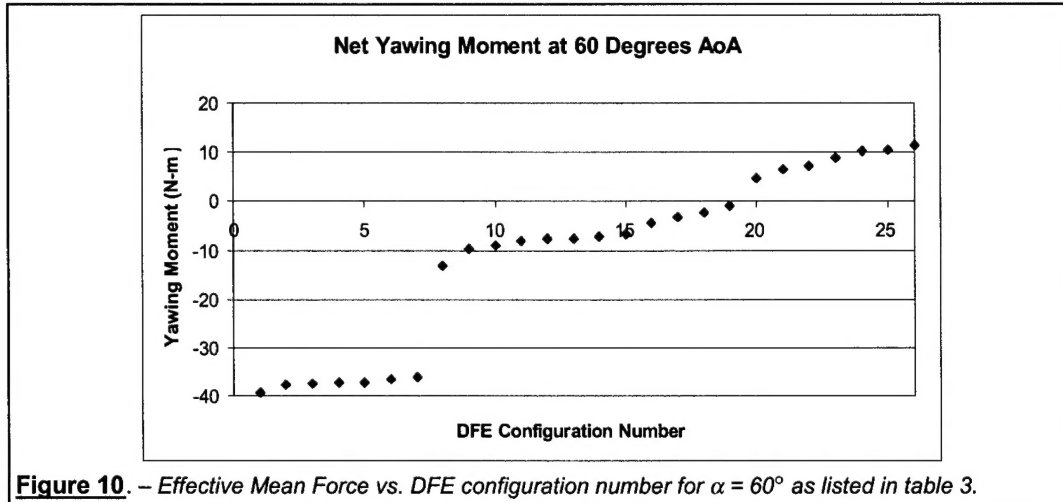
This is important since it shows the potential continuity of force production that may be achieved by cycling the flow effectors at different relative rates.

At a constant α , the effects of different DFE acutation for flow effectors 1 and 6 are studied. The effectiveness of the different DFE configuration number (see table 3) is noticeably demonstrated for $\alpha = 45^\circ$ in figure 7. Deploying flow effectors 1 and 6 at different frequencies as seen in figure 7 generates a wide spectrum of the mean force in the negative and the positive direction. Figure 8-10 show similar increase in the average yawing moment for a constant α versus different DFE configurations.

The pressure and the force balance data from the second sets of experiments are currently being analyzed. The pressure data can be used to estimate the orientation of the missile and to estimate the effective yawing moment on the missile at high α . The pressure data can track the formation of vortices that are entrained by the DFE's.

Summary

In this paper we present preliminary results for controlling asymmetric vortices shedding off a Missile nose cone through Deployable Flow Effectors developed by Orbital Research Inc. Flow control device designs (solid strakes and vortex generators) are evaluated with both passive and actively deployed strakes and vortex



generators on the forward surface of the missile. All the three flow control devices are evaluated with wind tunnel testing to determine the most effective design. Two mechanical devices (deployable strake and vortex generator row) are examined in forebody 2 and a single vortex generator device in forebody 1 in the first sets of experiments. Once the CLAS module is optimized for the location, size & shape of DFE's, CLAS rings consisting of 8 DFE's and 8 pressure sensors are integrated into the missile body for increased effectiveness and control of the vortices. The CLAS rings are capable of integrating MEMS for deployment of the flow effectors.

The first three flow effector designs are tested through a range of A's (up to 65°), circumferential body positions (CBP), and deployment heights to determine which design and configuration performed the best. For the range of α 's studied, the best position for the flow effectors placed in the

forebody 2 hatch are found to be 70° CBP while the best position for the flow effector placed in the forebody 1 (near nosecone) hatch is found to be 120° CBP. The second sets of experiments conducted with 8 DFE's integrated with 8 pressure sensors in the CLAS ring placed inside the missile nose cone demonstrates increased effectiveness in controlling the asymmetric vortices on the missile body. Most effective DFE's for $\alpha = 25^\circ$ to 40° are 0 & 5, $\alpha = 45^\circ$ & 50° are 1 & 6, and $\alpha = 55^\circ$ to 60° are 1 & 5 respectively.

Acknowledgements

This work is supported by, 1. Air Force Phase II SBIR "Active Flow Control for Aerodynamic Enhancement" Contract# F33615-99-3088, 2. Air Force Phase I SBIR "MEMS Actuated Deployable Strakes for Slender Bodies" contract #F08630-98-C-0033, and 3. Air Force Phase I SBIR "Smart Surface Fluid Flow Control Arrays" contract # F33615-98-C-3006.

References:

- ¹ Fisher, David F., Cobleigh, Brent R., "Controlling Forebody Asymmetries in Flight-Experience with Boundary Layer Transition Strips", NASA Technical Memorandum 4595, 1994.
- ² Ericsson, L.E., Reding, J.P., "Asymmetric Flow Separation and Vortex Shedding on Bodies of Revolution", Lockheed Missiles & Space Company, Inc., Sunnyvale, California 94088.
- ³ Cobleigh, Brent R. "High Angle of Attack Yawing Moment Asymmetry of the X-31

Aircraft from Flight Test", NASA Contractor Report 186030, 1994.

- ⁴ Ho, C.M., Tai, Y.C., "Review: MEMS and its Applications for Flow Control", Journal of Fluids Engineering, Vol. 118, September 1996, pp.437-447.
- ⁵ Favelukis, E.J., Lavine, A.S., Carman, G.P., "An Experimental Validated Thermal Model of Thin Film NiTi", Part of the SPIE Conference on Smart Surfaces and Integrated Systems, Newport Beach, California, March 1999.



DEPARTMENT OF THE AIR FORCE
HEADQUARTERS AIR ARMAMENT CENTER (AFMC)
EGLIN AIR FORCE BASE, FLORIDA

27 September 2000

MEMORANDUM FOR AFRL/MN CA-N

FROM: AAC/PA

SUBJECT: Clearance for Public Release (AAC/PA 00-422)

The technical paper titled "MEMS Actuated Deployable Flow Effectors System for Missile Control" has been reviewed. Public release is approved.

Jim I. Swinson
JIM I. SWINSON
Office of Public affairs

*Revised 4
1400
1 of 2*



DEPARTMENT OF THE AIR FORCE
AIR FORCE RESEARCH LABORATORY (AFRL)
EGLIN AIR FORCE BASE, FLORIDA

14 SEP 2000

MEMORANDUM FOR AAC/PA

FROM: AFRL/MN CA-N

SUBJECT: REQUEST FOR REVIEW AND CLEARANCE

1. Request review and approval of the attached paper for public release. Pertinent information is as follows:

- a. TITLE OF PUBLICATION: MEMS Actuated Deployable Flow Effectors System for Missile Control
- b. AUTHOR (S): Mehul P. Patel, T. Terry Ng, Frederick J. Lisy, Troy S. Prince, Jack M. DiCocco
- c. TITLE OF FORUM: AIAA Missile Sciences Conference
- d. SPONSOR: AIAA
- e. LOCATION AND DATE(S): Monterey CA, 7-9 Nov 00
- f. CLASSIFICATION OF CONFERENCE OR FORUM: Secret/US Citizen Only
- g. CLASSIFICATION OF PAPER: Unclassified
- h. FOREIGN NATIONALS WILL NOT BE PRESENT
- i. THE ABSTRACT/PAPER/PRESENTATION WILL be published in restricted unclassified proceedings available through the Defense Technical Information Center
- j. DEADLINE for submission: 17 Oct 00

2. The material contained in the attached paper is technically accurate, unclassified, and suitable for public release.

3. Even though key words that appear on the Militarily Critical Technologies List are included in the paper, the particular aspect of technology that the paper addresses is not included as part of the MCTL and will not result in the transfer of any militarily critical technology.

4. If you have any questions please contact Mike Valentino, AFRL/MNAV, 882-8878, EXT 3331.

FREDERICK A. DAVIS
Acting Chief Scientist
Munitions Directorate

Attachment:
MEMS Paper

*Review 4100
2092*